Detection and Management of Human-Cable Collision in Cable-Driven Parallel Robots

Hanbang Gao[1], Christine Chevallereau[1], and Stéphane Caro[1]

***Abstract*—This letter discusses the challenges and innovations in collision detection and management strategies for Cable-Driven Parallel Robots (CDPRs), focusing on enhancing safety in human-robot collaborative environments. A comprehensive collision management method is introduced. It integrates a novel method to detect collisions and identify the collided cable, leveraging tension sensor data and algorithmic strategies to improve accuracy and response to collision events. Adaptive management strategies for different collision severities, including minor and severe contacts, are presented, along with procedures for post-collision management. The methodologies are validated through experimentation with the CRAFT prototype, demonstrating their practical effectiveness. The findings have significant implications for the design and implementation of safety protocols in CDPRs.**

***Index Terms*—Tendon/Wire Mechanism, Parallel Robots, Human-Robot Collaboration, Physical Human-Robot Interaction, Safety in HRI.**

I. Introduction

AUTOMATION has significantly transformed industries with the advent of collaborative robots (cobots) in areas such as efficiently automotive production and rescue operations, demonstrating their adaptability and effectiveness [1], [2]. These cobots combine human expertise with robotic precision to enhance productivity and mitigate risks in hazardous tasks [3], [4].

In comparison to traditional robots, CDPRs offer a broader workspace and superior mass efficiency [5], aligning well with the concept of cobots. Nonetheless, safely integrating CDPRs into shared workspaces necessitates diligent consideration of physical Human-Robot Interaction (pHRI) and adherence to strict safety protocols [6], [7]. A significant challenge in this domain is human-cable collision, an area where most existing research focuses on avoidance strategies [8]–[10]. In [11]–[13], the authors explore the complexities of self-interference, specifically focusing on cable-cable and cable-object collisions. Additionally, [13]–[15] address issues related to known collision obstacles. Furthermore, [16] discusses the suitability, flexibility, and challenges of deploying CDPRs in complex environments where cable collisions are inevitable. However, a significant gap remains in addressing human-cable collisions, particularly in scenarios where the system operates autonomously without prior knowledge of potential collision situations.

Building upon the work presented in [17] on collision detection, this letter introduces a novel and comprehensive framework that integrates collision detection, cable identification, management, and post-collision recovery. This advancement enables more robust and flexible deployment of CDPRs in environments where human-cable interactions are unpredictable. The main contributions of this letter are threefold:

- **Collision Detection**: This letter presents two distinct methodologies for collision detection.
- **Cable Collision Identification**: It addresses the challenge of determining the collided cable and proposes a mathematical model that utilizes both measured and desired cable tensions.
- **Collision Management**: It details two distinct management strategies for effectively addressing both minor and severe collisions.

Each phase of this entire framework has been validated through comprehensive experiments.

The organization of this letter is as follows: Section I presents the experimental setup, the control scheme, and the trajectory planning. Section II discusses collision detection by evaluating discrepancies in cable tension measured against a specified threshold. Section III outlines the proposed methodology for identifying the collided cable. In Section IV, collisions are categorized into minor and severe based on the estimation of the equivalent force exerted on the platform. Section V presents specific control strategies for each category, designed to reduce cable tension and enhance operator safety. Section VI addresses the post-collision phase, focusing on detecting collision ends and facilitating system recovery. The conclusions and future work are summarized in Section VII.

A. Experimental setup

The CRAFT platform is a CDPR experimental prototype at LS2N. The CRAFT prototype has eight cables leading to eight loop-closure equations. Each loop integrates a winch unit, a guiding pulley, and a cable that connects to the Moving Platform (MP). Fig. 1 illustrates one complete actuation chain in the CRAFT prototype. In the setup, the cable is wound around the drum and then passes through the pulley before being attached to the MP anchor point. In this configuration,

Manuscript received: May 10, 2024; Revised August 18, 2024; Accepted October 8, 2024; date of current version October 17, 2024. This letter was recommended for publication by Editor G. Venture and Editor-in-Chief T. Asfour upon evaluation of the Reviewers' comments. This work was supported by both ROBOTEX 2.0 (Grants ROBOTEX ANR-10-EQPX-44-01) and TIRREX (ANR-21-ESRE-0015). (Corresponding author: Stéphane Caro).

[1]Nantes Université, École Centrale Nantes, CNRS, LS2N, UMR 6004, F-44000 Nantes, France. {hanbang.gao, christine.chevallereau, stephane.caro}@ls2n.fr

Digital Object Identifier (DOI): 10.1109/LRA.2024.3487051.

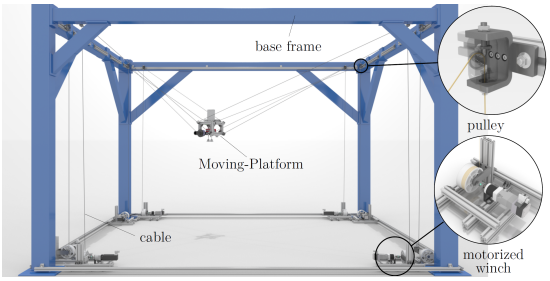

Fig. 1. Scheme of CRAFT Prototype [18]

the cable, wound around the drum, passes through the pulley before attaching to the MP anchor point.

The CRAFT platform operates through a system where a main computer (the supervision PC) communicates with a real-time computer using dSPACE, which in turn directs the desired torque to the eight motors, ensuring the whole system works together smoothly. Two key types of measurements are derived from the system: 1) motor encoders send the motors joint angles $\mathbf{q}$ to the real-time PC; 2) dynamometers, positioned near the cable attachment points, transmit cable tension data $\boldsymbol{\tau}_m$ to the real-time PC. Both types of sensors are synchronized at a frequency of 1000 Hz.

B. Control Scheme of CRAFT

The control scheme of the CRAFT prototype, depicted in Fig. 2, integrates three main components in different color patches. Its objective is to achieve the desired MP pose $\mathbf{p}_d$, twist $\mathbf{v}_d$, and twist derivative $\dot{\mathbf{v}}_d$. This is accomplished by applying the control output torque $\boldsymbol{\Gamma}_{mg}$ on the motor and gearbox assembly. This torque is a combination of $\boldsymbol{\Gamma}_c$ (represented by the blue patch) and $\boldsymbol{\Gamma}_d$ (represented by the green patch), which respectively represent the control torques acting on joint space for motor positioning and Cartesian space for platform movement. A saturation filter limits this combined torque to safeguard the motor-gearbox from excessive forces, ensuring operational integrity. The red patch represents the collision management Strategy 1.

Specifically, $\boldsymbol{\Gamma}_c$ is the torque required to move the motor to their expected position, following a computed torque control law that includes Proportional-Integral-Derivative (PID) corrector of the motor joint based on angular positions $\mathbf{q}$ and their desired values $\mathbf{q}_d$. The PID corrector employs gains K_p, K_i, and K_d and is formulated considering the Inverse Geometric Elasto-static Model (IGEM) [19]. IGEM, taking into account pulleys' geometry and cables' elasticity, allows for precise control by calculating each motor's motion required to move the MP as desired. The close-loop tracking error for wrench joint position is $\mathbf{e} = \mathbf{q}_d - \mathbf{q}$. The PID corrector aims to minimize this error such that:

$$\ddot{\mathbf{e}} + K_d\ \dot{\mathbf{e}} + K_p\ \mathbf{e} + K_i \int \mathbf{e}\, dt = 0 \tag{1}$$

Thus the corresponding acceleration of the motor joint is:

$$\ddot{\mathbf{q}} = \ddot{\mathbf{q}}_d + K_d\ (\dot{\mathbf{q}} - \dot{\mathbf{q}}_d) + K_p\ (\mathbf{q} - \mathbf{q}_d) + K_i \int (\mathbf{q} - \mathbf{q}_d)\, dt \tag{2}$$

The torque $\boldsymbol{\Gamma}_c$ required to produce this acceleration must also compensate the Coulomb viscous friction modelled with static $\mathbf{f}_s$ and fluid $\mathbf{f}_v$ friction terms:

$$\boldsymbol{\Gamma}_c = \mathbf{I}_m \ddot{\mathbf{q}} + \mathbf{f}_s \odot \operatorname{sign}(\dot{\mathbf{q}}_d) + \mathbf{f}_v \odot \dot{\mathbf{q}}_d, \tag{3}$$

where $\mathbf{I}_m$ is the inertia matrix of the motor and gearbox, and $\mathbf{a} \odot \mathbf{b}$ represents the element-wise multiplication of vectors $\mathbf{a}$ and $\mathbf{b}$.

$\boldsymbol{\Gamma}_d$ determines the required motor torques to enable the MP to track the operational trajectories by providing the desired cable tensions $\boldsymbol{\tau}_d$. This process utilizes a feed-forward element, $\mathbf{w}_{ext}$, derived from the Inverse Dynamic Model (IDM). The IDM compensates for system dynamics, including inertia, Coriolis forces, and gravitational effects, without requiring external measurements of the MP's pose, velocity, and acceleration:

$$\mathbf{w}_{ext} = \mathbb{I}_p \dot{\mathbf{v}}_d + \mathbf{C}\mathbf{v}_d - \mathbf{w}_e - \mathbf{w}_g, \tag{4}$$

where $\mathbb{I}_p$ represents the MP inertia tensor, and $\mathbf{C}$, $\mathbf{w}_e$, and $\mathbf{w}_g$ are the Coriolis matrix, external wrench on the MP, and gravity wrench, respectively. This approach provides a predictive model of the wrench required for desired MP motions. Desired cable tensions $\boldsymbol{\tau}_d$ are then optimized via quadratic programming to choose tension distribution within operational limits:

$$\begin{aligned} &\underset{\boldsymbol{\lambda}}{\operatorname{argmin}} \left\| \boldsymbol{\tau}_d \right\|^2, \\ &\text{subject to} \quad \boldsymbol{\tau}_{\min} \leq \boldsymbol{\tau}_d \leq \boldsymbol{\tau}_{\max}. \end{aligned} \tag{5}$$

In this analysis, $\boldsymbol{\tau}_{\min}$ represent the minimum cable tension vectors, each component set to 1 N, ensuring that the cable remains taut. Conversely, $\boldsymbol{\tau}_{\max}$ denotes the maximum cable tension, that is set at 100 N for each component in accordance with cable safety guidelines. Furthermore, $\boldsymbol{\tau}_d$ is defined as a function of the two-dimensional vector $\boldsymbol{\lambda}$, as follows:

$$\boldsymbol{\tau}_d = -\mathbf{W}_d^{\dagger}\ \mathbf{w}_{ext} + \mathbf{N}_d\ \boldsymbol{\lambda}, \tag{6}$$

where $\mathbf{W}_d$ is the desired wrench matrix of CDPRs based on IGEM model. The symbol † denotes the Moore-Penrose pseudo-inverse of the wrench matrix, and $\mathbf{N}_d$ is a matrix projecting onto the kernel of the wrench matrix, such that $\mathbf{W}_d\ \mathbf{N}_d\ \boldsymbol{\lambda} = \mathbf{0}_6$, and r_d is the winch radius. From (2) - (6), control input in terms of motor torques is expressed as:

$$\boldsymbol{\Gamma}_{mg} = \operatorname{sat}(r_d \boldsymbol{\tau}_d + \boldsymbol{\Gamma}_c), \tag{7}$$

where $\operatorname{sat}(\cdot)$ denotes the saturation function.

C. Experimental Trajectory

In the collision experiments with the CRAFT prototype, a planned trajectory is designed that navigates largely through the robot's feasible workspace, incorporating both translational and rotational dynamics. A 60-second trajectory is split into eight phases, designed for smooth acceleration without abrupt changes. It follows the robotic preference for a fifth-order polynomial motion plan. This method facilitates the control

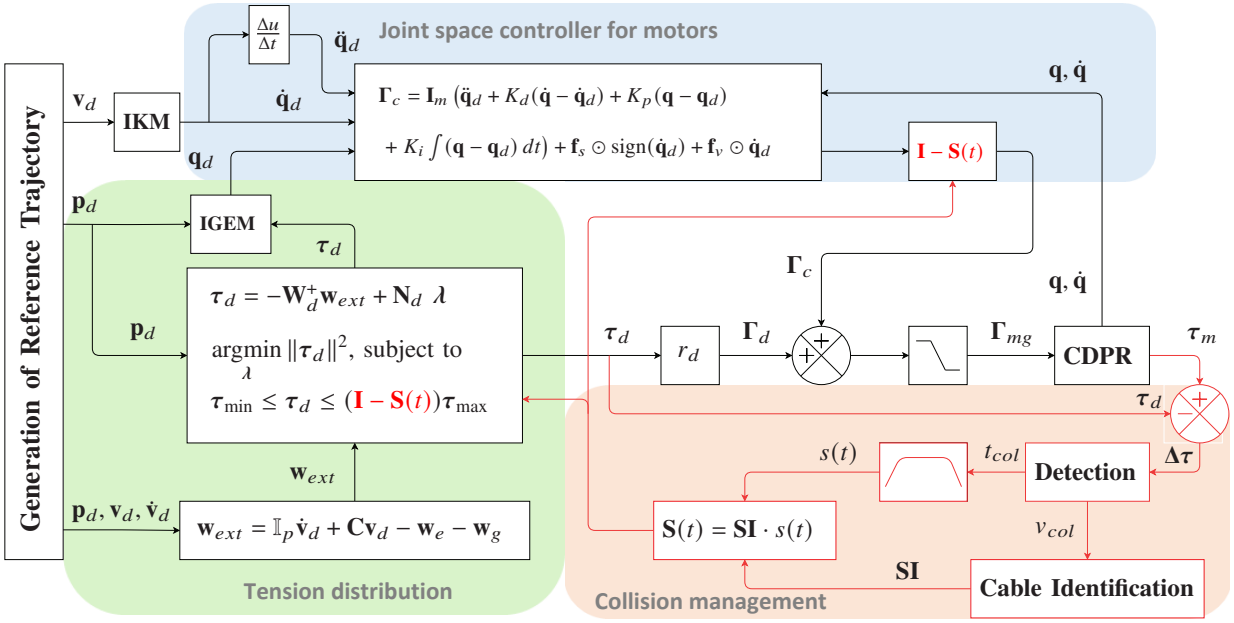

Fig. 2. Control scheme of the CRAFT platform: the black components represent the standard operational control scheme without collision management. In contrast, the red components introduce the collision management Strategy 1, highlighting modifications activated in response to collision events.

of position, velocity, and acceleration of the MP, ensuring seamless transitions between phases.

II. Collision Detection

This letter focuses on managing collisions between CDPR cables and human operators. Collision detection can be achieved by monitoring the distance between cables and operators. Although motion capture systems are effective, they suffer from issues such as occlusion, low frequency, and the need for initial calibration. Capacitive cables, introduced for proximity detection in [20], add to the cable mass, which, as discussed in [13], contributes to increased sagging and reduced accuracy. In contrast, cable tension sensors are straightforward to install and versatile in application, making them the preferred choice for the experiments.

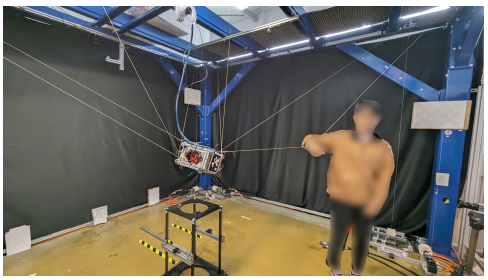

Fig. 3. Collision test between a human operator and a cable on the CRAFT platform [2].

Figure 3 depicts a collision test involving a human operator and one cable of a CDPR. This interaction leads to a noticeable variation in cable tension, as recorded by a force sensor attached to the anchor point on the MP. When a collision occurs, the tension in the collided cable increases relative to its reference tension. If this increment exceeds a certain threshold, occurrence of a collision can be detected. The calibration of this threshold is critical due to the force sensor's inherent measurement oscillations. If the threshold is set too small, it may erroneously detect collisions even when none have actually occurred. The cable force measurement value, directly obtained from dynamometers, is defined as $\boldsymbol{\tau}_m$. To effectively determine cable collisions, the desired cable tensions $\boldsymbol{\tau}_d$ are utilized as the reference tensions. The reference tension is produced by the tension distribution algorithm as illustrated in (6). The value of $\boldsymbol{\tau}_d$ solely depends upon the predefined trajectory, rendering it unaffected by collisions. Here, the tension tracking error $\boldsymbol{\Delta\tau}$ is defined as an 8×1 vector, representing the difference between the desired and measured cable tensions.

$$\boldsymbol{\Delta\tau} = \boldsymbol{\tau}_m - \boldsymbol{\tau}_d \tag{8}$$

A threshold of 5 N has been empirically determined, balancing sensitivity and specificity in collision detection, supported by findings in [17].

$$\mathrm{T}_h = 5\,\mathrm{N} \tag{9}$$

Therefore, a collision is determined if there exists at least one element $\Delta\tau_i$ in $\boldsymbol{\Delta\tau}$ such that $\Delta\tau_i > 5\,\mathrm{N}$. This condition can be written as:

$$\exists\, \Delta\tau_i \in \boldsymbol{\Delta\tau} : \Delta\tau_i > \mathrm{T}_h \tag{10}$$

Figure 4 illustrates the collision experiment, following the predefined trajectory. At 31.873 s, a collision occurs, and the threshold T_h is surpassed at 32.128 s, indicating at least one cable has been impacted. This is visually represented by the intersection of the threshold line with the magenta line, corresponding to cable 8. The interval between collision occurrence and detection time is 0.255 s, demonstrating the

[2]The experiment videos are available at https://youtu.be/719kyfrKlI4.

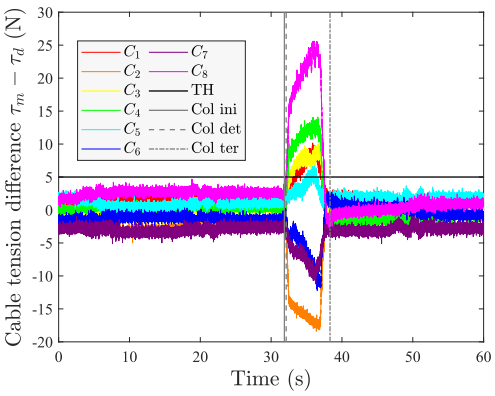

Fig. 4. Difference between measured and desired cable tensions during a collision event from 31.873 s to 38.317 s. Here, C_j denotes the j^{th} cable of the CDPR, $j = 1, 2, \ldots, 8$; 'TH' represents threshold T_h; 'Col' stands for collision; 'ini' for initialization; 'det' for detection; and 'ter' for termination.

system's prompt collision detection capability.

From Fig. 4, it is observed that the cable tension errors $\boldsymbol{\Delta\tau}$ vary and oscillate around ± 2 N. This fluctuation is due to the measurement error of dynamometers. To avoid delay and save computing time for such a high-frequency system (1000 Hz), direct measurements from sensors are used without filtering. However, the cable tension errors range from ± 4.5 N rather than ± 2 N when there is no collision, stemming from two sources. First, feed-forward control is implemented to manage cable tension and relies heavily on the accuracy of the modeling since it does not incorporate feedback. However, subtle errors in the parameters of CDPR components such as pulleys, cables, and MP are introduced. Specifically, the cable is considered massless, and its elongation is proportional to its modulus of elasticity. These assumptions impact the accuracy of the model. When these parameters, including the assumptions about the cables, are used as predefined terms in (4) and (6), it results in inaccuracies in the cable tension control, leading to increased tension tracking errors and affecting the threshold for the experiment. Second, the communication cable (the blue cable in Fig. 3) moves inevitably with the MP. The upper part of the cable is wired on a large pulley and then connected to a PC, but the remaining part from the pulley to the MP, with its mass changing as the trajectory progresses and acts as a small variable payload on the MP, which so far has not been well modeled.

III. Cable Collision Identification

A. Problem Statement

The aim of cable collision identification is to identify the specific cable involved in the collision as it occurs. While collisions between a human and the MP can be detected by the F/T sensors assembled on the MP, this study focuses on scenarios where a single cable of the CDPR collides with a human operator. As illustrated in Fig. 4, when a collision occurs between the environment and a specific cable, experimental results indicate variations in all cable tensions.

The first heuristic method assumes that upon detecting a collision, the cable with the highest difference is the one that has collided. The reasoning is simple: an external force applied to the struck cable modifies its shape and the tension in the cable. However, these conditions are reflected on the MP, influencing the tension in all other cables. It cannot be guaranteed that the collided cable will have the greatest increase in tension. For instance, Fig. 5 illustrates the case of collisions with cable 8 around time 10 s, cable 4 around time 30 s, and cable 7 around time 50 s. This heuristic method works fine for cable 7, as $\Delta\tau_7$ first reaches T_h and has the highest cable tension during the collision.

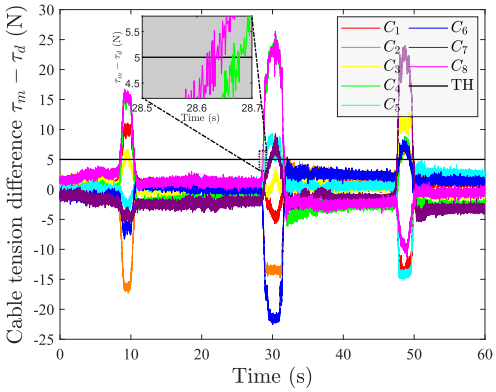

Fig. 5. Difference between the measured and desired cable tensions: collision first with cable 8, then with cable 4, last with cable 7.

However, this method works for the first collision observed, involving cable 8 (magenta line), but not for the second collision involving cable 4 (highlighted in green). Notably, in each instance of collision, cable 8 invariably reaches the 5 N threshold prior to cable 4, maintaining a tension level consistently surpassing that of cable 4. This scenario presents a risk of misidentifying the collision as involving cable 8 instead of the actual cable 4. Upon conducting similar experiments, the diagonal cable pairs are often misidentified. Thus, precise identification of the specific collided cable is essential for effective collision management.

B. Cable Identification Criteria

In order to solve the identification problem, an enhanced set of criteria is proposed, informed by comprehensive collision modeling, to more accurately identify the specific cable involved in a collision.

Assumption 1: The collision can be regarded as pulling effects on the c^{th} cable. The collision will alter the shape of the impacted cable. Thus it will affect the direction of the force applied on the MP by this cable.

Assumption 2: The system remains controllable and stable during the collision, with the MP maintaining stability in its trajectory despite possible minor orientation changes.

The (3×8) matrix $\mathbf{U}$ is defined, where each column is composed of the unit vector indicating the direction of the respective cable. Specifically, the matrix $\mathbf{U}_d = [\mathbf{u}_{1d}, \mathbf{u}_{2d}, \ldots, \mathbf{u}_{8d}]$ comprises the desired unit vectors, while $\mathbf{U}_r = [\mathbf{u}_{1r}, \mathbf{u}_{2r}, \ldots, \mathbf{u}_{8r}]$ combines the actual unit vectors. Figure 6 illustrates the scheme of the collision geometry

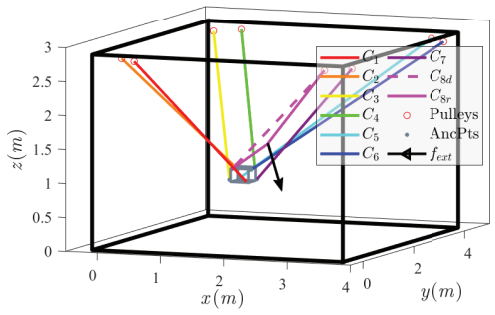

Fig. 6. Geometry effects due to collision between cable 8 and the environment

effects of a single cable collision. The fundamental concept behind cable collision identification hinges on the fact that only the collided cable has a shape change under the assumption that the MP stays at the desired pose. Let $\mathbf{u}_{jd}$ and $\mathbf{u}_{jr}$ represent the j^{th} column of $\mathbf{U}_d$, and $\mathbf{U}_r$, respectively. If just one cable collides, it will change only the displacement of the collided cable denoted c. Thus, $\mathbf{U}_d$ and $\mathbf{U}_r$ have the following relation:

$$\mathbf{u}_{cd} \neq \mathbf{u}_{cr}, \tag{11}$$

$$\mathbf{u}_{id} = \mathbf{u}_{ir}, \quad i = 1, 2, ..., 8 \quad \textbf{and} \quad i \neq c \tag{12}$$

The value of the desired cable unit vector $\mathbf{u}_{id}$ can be calculated through IGEM of CDPRs and the desired pose of the MP.

Due to *Assumption* 2, which states that variations in cable tensions do not affect the tracking capabilities of the MP in position, it is concluded that the impact of cable tension on the platform is effectively negligible, equivalent to zero. The impact of cable tension variation is represented as the wrench matrix multiplied by the difference in cable tension.

$$\mathbf{U}_r \boldsymbol{\Delta\tau} = \mathbf{0}_3 \tag{13}$$

Although the actual directions of the cables remain unknown, (12) allows us to rewrite (13). This new form assumes that cables not directly involved in a collision maintain their desired direction:

$$\sum_{i=1,\ i\neq c}^{8} \mathbf{u}_{id}^T \Delta\tau_i = -\mathbf{u}_{cr} \cdot \Delta\tau_c, \tag{14}$$

where $\Delta\tau_i$ represents the i^{th} component of $\boldsymbol{\Delta\tau}$. Therefore, the magnitude of the sum of forces on all uncollided cables should be equal to the magnitude of the tension change in the affected cable:

$$\left| \sum_{i=1,\ i\neq c}^{8} \mathbf{u}_{id}^T \Delta\tau_i \right| = |\Delta\tau_c| \tag{15}$$

To identify the specific cable that experienced the collision, a function $g(x)$ is defined:

$$g(x) = \left| \left| \sum_{i=1,\ i\neq x}^{8} \mathbf{u}_{id}^T \Delta\tau_i \right| - |\Delta\tau_x| \right| \tag{16}$$

The function $g(x)$ achieves its minimum value, which is 0, when $x = c$. c is the collided cable index.

C. Results and Analysis

Incorporating the hypothesis that a collision involving a cable is characterized by a simultaneous increase in tension $\boldsymbol{\Delta\tau}$, and a rise in $g(x)$, the identification methodology is refined through a composite criterion. The procedure initiates by monitoring deviations between the current cable tension and a predefined reference tension. When a difference exceeds a specified threshold is observed, the two cables exhibiting the most significant tension differences are recorded. Subsequently, focus is shifted towards the two cables demonstrating the smallest $g(x)$ at that moment. The intersection of these assessments enables the identification of the cable involved in the collision. This strategy effectively combines tension difference and the minimization of geometric errors, thereby enhancing the precision in identifying the correct cable involved in a collision and reducing the likelihood of misidentification based on a single criterion alone.

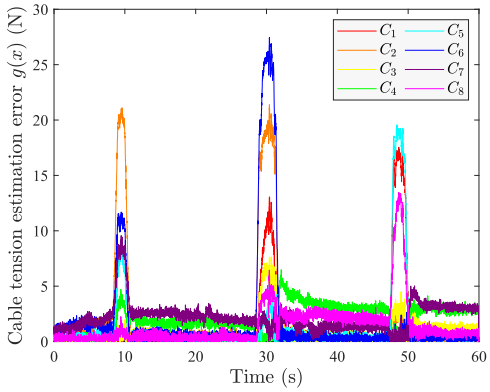

Fig. 7. Estimated tension errors for all cables, collision first with cable 8, then with cable 4, last with cable 7.

Figure 7 displays the estimated tension errors $g(x)$ for all cables associated with the collision scenario shown in Fig. 5. Cables 8, 4, and 7 exhibit the lowest $g(x)$ values. By applying the cable identification procedures described in Table I, the results accurately reflect the sequence of collisions as they occur.

TABLE I
CABLE IDENTIFICATION RESULTS FOR COLLISION SEQUENCES

Sequences	**Largest** $\Delta\tau$	**Smallest** $g(x)$	**Results**
1st Col	$C_8 > C_4$	$C_8 < C_1$	C_8
2nd Col	$C_8 > C_4$	$C_4 < C_5$	C_4
3rd Col	$C_7 > C_3$	$C_7 < C_6$	C_7

IV. Collision Classification

In scenarios involving cable-human collisions, these incidents are categorized as feasible or non-feasible. Feasibility refers to whether the pose can be maintained with zero tension in the collided cable. Collisions may also vary based on the magnitude of the contact force, ranging from minor, falling within acceptable limits, to severe, potentially posing a safety risk to the operator.

The effects of the external force $\mathbf{f}_{ext}$ acting on collided cable could be equal to one equivalent force $\mathbf{f}_{eq}$ exerted on the MP during a collision, which can be approximately calculated as:

$$\mathbf{f}_{eq} = \begin{cases} \mathbf{U}_d \boldsymbol{\Delta\tau}, & \text{if no collision} \\ \sum_{j=1,\ j\neq c}^{8} \mathbf{u}_{jd}\ \Delta\tau_j & \text{if cable } c \text{ collides} \end{cases} \tag{17}$$

In (17), the effects of the collided cable are not considered when a collision occurs, as $\mathbf{u}_{cd}$ significantly differs from $\mathbf{u}_{cr}$. Including the collided cable terms would lead to larger errors.

Furthermore, these terms are relatively minor at the end of the collision, making them useful criteria for detecting its termination. If $\mathbf{f}_{eq}$ exceeding a specific threshold, here set at 10 N, is classified as a severe collision. Conversely, any value below this threshold indicates a minor collision.

V. Collision Management

In the event of a collision involving a single cable, the management strategy aims to reduce the cable tension to the minimum cable tension. This action, premised on identifying the cable in collision, nullifies the contact force on human operators, mitigating injury risk.

A. Strategy 1: Managing Minor Collisions

Using the previously outlined collision classification, a strategy for minor collisions is designed. This strategy is to reduce the cable tension on the collided cable. Execution within a viable MP workspace is crucial, as it allows tension adjustment of the impacted cable to the minimum allowed tension. It is important to note, however, that this proposed solution is currently limited to scenarios occurring within this feasible workspace. Collisions that occur outside of this defined workspace present complexities that warrant further investigation, which is planned for future research.

The red block in Fig. 2 shows the safety management strategy for minor collisions. Upon detection and cable identification of a collision, the strategy involves a gradual reduction of the maximum tension distribution. Simultaneously, joint space feedback control, $\boldsymbol{\Gamma}_c$ on the collided cable is progressively restricted. The collision management procedures are defined as follows:

1) Upon collision detection, the red detection block in Fig. 2 outputs a vector $\mathbf{v}_{col}$, which provides the cable tension profile at the collision time $\mathbf{t}_{col}$. To model the tension evolution in the collided cable, a function $s(t)$ is defined to quantify the proportion of maximum tension over the 5-second management duration, which is chosen to avoid a sudden reduction in control input and ensure a gradual decrease in tension. Subsequently, a cable selector $\mathbf{SI}$ is utilized to differentiate between collided and normally operating cables through the cable identification algorithm.
$$\mathbf{SI} = \text{diag}(\delta_{1,c}, \delta_{2,c}, \ldots, \delta_{8,c}), \tag{18}$$
where the Kronecker delta, $\delta_{i,j}$, is defined as 1 when $i = j$ and 0 otherwise.
2) The management time function, $\mathbf{S}(t)$, is obtained by the dot product of $s(t)$ and $\mathbf{SI}$. This function is then used to decrease the maximum cable tension $\boldsymbol{\tau}_{\max}$ until it reaches $\boldsymbol{\tau}_{\min}$. Simultaneously, the control parameter, $\boldsymbol{\Gamma}_c$ is also gradually reduced to zero.
3) Following the detection of collision resolution, the function $\mathbf{S}(t)$ is updated. Contrary to the process described in step 2, this revised function is employed to incrementally restore the maximum cable tension, $\boldsymbol{\tau}_{\max}$, and the control parameter, $\boldsymbol{\Gamma}_c$, to their nominal values.

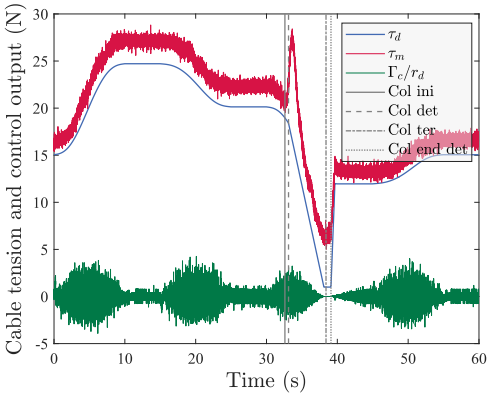

Fig. 8. Evolution of cable 8 tension and collision response with collision management Strategy 1 for minor collisions

As depicted in Fig. 8, a marked escalation in cable tension $\tau_{m,8}$ (red line) is detected at 32.600 s, signaling a collision with cable 8. Collision is subsequently detected at 33.111 s, precipitating a prompt reduction in the desired cable tensions to 1 N. Over time, the amplitude of the corrector output (green line) for the collided cable shows a gradual decline. The measured tension of the collided cable is reduced to around 5 N. After detecting the end of the collision, the cable tension recovers to the desired level, and the control output gradually resumes. The results can be seen in Experiment 1 of the supplementary video.

B. Strategy 2: Managing Severe Collisions

Strategy 1, while effective for managing minor cable collisions, reveals its limitations when the system encounters ongoing or severe external forces. Under such conditions, the tension in the cable inevitably rises due to the non-reversibility of the servo motor, which cannot reverse the cable's direction to counter the force.

Figure 9 demonstrates the shortcomings of Strategy 1 in addressing severe collisions, as presented in Experiment 2 of the supplementary video. Even after fully suppressing the

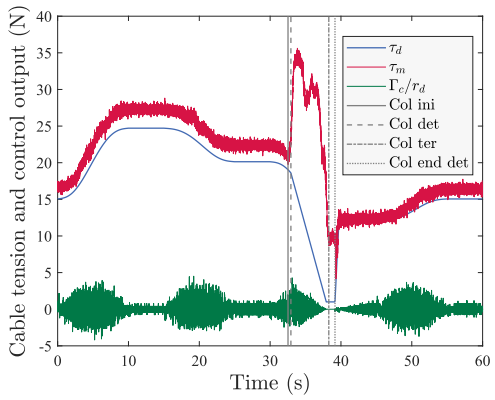

Fig. 9. Evolution of cable 8 tension and collision response with collision management Strategy 1 for severe collisions

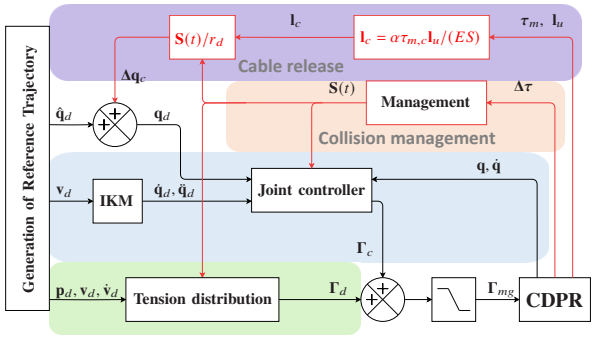

Fig. 10. Enhanced control scheme of the CRAFT platform: this scheme extends the control scheme shown in Fig. 2 by introducing additional improvements. It includes a method to release the collided cable by adjusting the desired cable length (the purple patch), while maintaining the cable tension reduction technique initially introduced in Strategy 1.

PID output and lowering the desired cable tension to 1 N, the cable tension remains unmitigated after 5 seconds of management. It can be concluded that simply reducing the desired tension is insufficient; actively elongating the cable by moving the motor becomes necessary to relieve the tension. In light of this, the letter suggests an adjustment of the desired motor joint positions, $\mathbf{q}_d$, to facilitate intentional cable slack, preventing external forces from further increasing the tension. This modification should be adequate to avoid complicating the subsequent post-collision recovery phase. The optimal extent of cable elongation $\mathbf{l}_c$ can be dynamically computed based on the tension increment and the MP's position when collision is just detected. Utilizing the properties of an ideal elastic cable, it can be obtained:

$$\mathbf{l}_c = \frac{\alpha\ \tau_{m,c}\ \mathbf{l}_u}{ES}, \tag{19}$$

where E denotes the Young's modulus of the cable material, and S represents the cable's cross-sectional area. The axial stiffness (ES) is determined using a cable identification experimental apparatus rather than relying on the manufacturer's value. The errors in estimation would negatively impact the accuracy of the released cable. The vector $\mathbf{l}_u$ contains the cable lengths from the cable anchor points, which can be measured by the motor encoders. The measured cable tension of the collided cable is denoted as $\tau_{m,c}$. The factor α is a safety factor, chosen to be 1.5.

Strategy 2 (Fig. 10) builds upon the foundation of Strategy 1 (Fig. 2) by incorporating adaptive cable length adjustment, allowing the system to more effectively handle higher levels of tension and enhancing its robustness in response to severe collisions. Upon the detection and confirmation of a collision affecting a specific cable, the proposed Strategy 2, applicable within the adaptive cable elongation, entails a gradual extension of the joint angle to $\boldsymbol{\Delta}\mathbf{q}_c + \hat{\mathbf{q}}_d$. This deliberate maneuver aims to reduce tension in the collided cable, thereby decreasing potential risks to human operators.

Upon comparing Fig. 8 with Fig. 11, an observable escalation in the desired cable tensions, highlighted by the red line, indicates the occurrence of a more severe collision. Nonetheless, the adjustment in the desired joint position leads to a

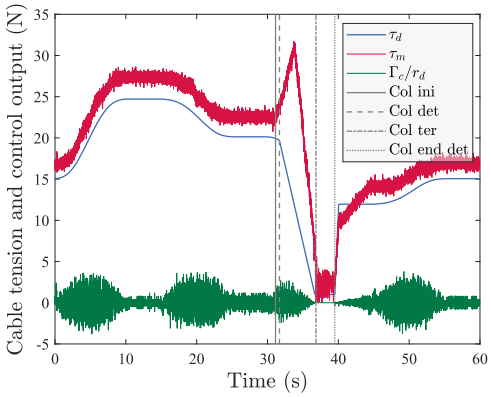

Fig. 11. Evolution of cable 8 tension and collision response with collision management Strategy 2 for severe collisions

reduction in cable tension, albeit accompanied by oscillations due to the sagging effect. It illustrates the effectiveness of the enhanced control strategy, Strategy 2, in mitigating the adverse effects of severe collisions, building on the foundation established by Strategy 1.

VI. Post-Collision

In the post-collision phase, the objective is to detect the end of the collision and subsequently facilitate system rehabilitation. The reference cable tension values $\boldsymbol{\tau}_d$, adjusted during the management phase, are no longer reliable indicators for detecting the end of the collision. An alternative method, employing (17), is proposed. This equation provides an approximate assessment of the equivalent force, $\mathbf{f}_{eq}$. A collision is considered to have ended when the magnitude of $\mathbf{f}_{eq}$ remains below 5 N for a continuous duration of one second. For collision management Strategy 2 and detection of the end of the collision, refer to Experiment 3 in the supplementary video, where the reaction process is shown in detail.

For CDPR restoration, the desired cable tensions are gradually restored to the values without collision and PID corrector outputs are unblocked. When applying Strategy 2, adjusting desired joint angle is vital for maintaining system integrity

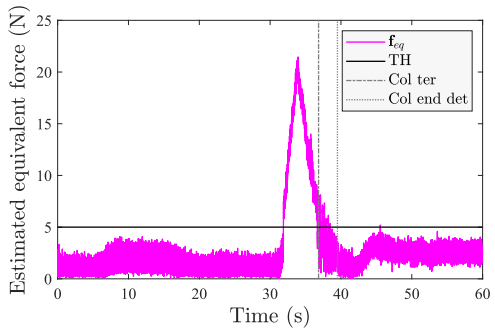

Fig. 12. Equivalent force $\mathbf{f}_{eq}$ with the collision management strategy for cable 8, referring to collision case in Fig. 11, where the collision ends around 36.980 seconds and is detected at 39.503 seconds.

and restore normal state. These steps are crucial for ensuring CDPR durability in collision-prone environments.

VII. Conclusion

This letter introduces a comprehensive framework for managing human-cable collisions in CDPR, incorporating detection, cable identification, and management strategies. It highlights the challenges of traditional detection methods based on tension discrepancies, proposing a novel cable identification strategy supported by a mathematical model. Additionally, the detection of the end of the collision relies on estimating the equivalent force exerted on the MP due to cable-human collisions. The effectiveness of two distinct management approaches for minor and severe collisions is demonstrated through practical experiments. These contributions highlight the potential of the approach to improve human-CDPR collaboration safety.

This letter studies human-cable collisions, and the method could be extended to human-platform and cable-cable collisions, which will require further testing and comparison with existing methods. Future research will focus on managing human-cable collisions outside the feasible workspace. In these scenarios, it is not feasible to reduce the tension in the collided cable while allowing the collision to continue. Since the actual pose of the robot cannot be maintained, an escape trajectory will be developed through path planning, adjusting the trajectory based on the position of the obstacle, to guide the system back to a feasible workspace and enable cable release. To implement this method effectively, it will be necessary to gather more detailed information about collisions. Efforts will focus on developing collision models that accurately reconstruct collision scenarios involving human-robot physical interactions, by determining the positions and directions of external forces during these events. Those contributions will support the development of advanced safety and efficiency measures for CDPRs in collaborative environments, ensuring effective and secure human-robot interaction.

Acknowledgment

This work was supported by both ROBOTEX 2.0 (Grants ROBOTEX ANR-10-EQPX-44-01) and TIRREX (ANR-21-ESRE-0015). The first author is funded by the China Scholarship Council (Grant no. 202208070012). Assistance provided by M. Marceau Métillon through the experiments is highly appreciated.

References

[1] M. Javaid, A. Haleem, R. P. Singh, and R. Suman, "Substantial capabilities of robotics in enhancing industry 4.0 implementation," *Cognitive Robotics*, vol. 1, pp. 58–75, 2021.

[2] A. P. Calitz, P. Poisat, and M. Cullen, "The future african workplace: The use of collaborative robots in manufacturing," *SA Journal of Human Resource Management*, vol. 15, no. 1, pp. 1–11, 2017.

[3] G. Ferri*, A. Munafò*, A. Tesei, P. Braca, F. Meyer, K. Pelekanakis, R. Petroccia, J. Alves, C. Strode, and K. LePage, "Cooperative robotic networks for underwater surveillance: an overview," *IET Radar, Sonar & Navigation*, vol. 11, no. 12, pp. 1740–1761, 2017.

[4] M. A. Díaz, M. Voß, A. Dillen, B. Tassignon, L. Flynn, J. Geeroms, R. Meeusen, T. Verstraten, J. Babič, P. Beckerle *et al.*, "Human-in-the-loop optimization of wearable robotic devices to improve human–robot interaction: A systematic review," *IEEE Transactions on Cybernetics*, 2022.

[5] S. Qian, B. Zi, W.-W. Shang, and Q.-S. Xu, "A review on cable-driven parallel robots," *Chinese Journal of Mechanical Engineering*, vol. 31, no. 1, pp. 1–11, 2018.

[6] J. Garrido, D. Silva-Muñiz, E. Riveiro, J. Rivera-Andrade, and J. Sáez, "Collaborative behavior for non-conventional custom-made robotics: A cable-driven parallel robot application," *Machines*, vol. 12, no. 2, p. 91, 2024.

[7] M. Métillon, C. Charron, K. Subrin, and S. Caro, "Performance and interaction quality variations of a collaborative cable-driven parallel robot," *Mechatronics*, vol. 86, p. 102839, 2022.

[8] J.-H. Bak, S. W. Hwang, J. Yoon, J. H. Park, and J.-O. Park, "Collision-free path planning of cable-driven parallel robots in cluttered environments," *Intelligent Service Robotics*, vol. 12, pp. 243–253, 2019.

[9] E. Khoshbin, K. Youssef, R. Meziane, and M. J.-D. Otis, "Reconfigurable fully constrained cable-driven parallel mechanism for avoiding collision between cables with human," *Robotica*, vol. 40, no. 12, pp. 4405–4430, 2022.

[10] Y. Liu, Z. Cao, H. Xiong, J. Du, H. Cao, and L. Zhang, "Dynamic obstacle avoidance for cable-driven parallel robots with mobile bases via sim-to-real reinforcement learning," *IEEE Robotics and Automation Letters*, vol. 8, no. 3, pp. 1683–1690, 2023.

[11] R. Meziane, P. Cardou, and M. J.-D. Otis, "Cable interference control in physical interaction for cable-driven parallel mechanisms," *Mechanism and Machine Theory*, vol. 132, pp. 30–47, 2019.

[12] D. Q. Nguyen and M. Gouttefarde, "On the improvement of cable collision detection algorithms," in *Cable-Driven Parallel Robots: Proceedings of the Second International Conference on Cable-Driven Parallel Robots*. Springer, 2015, pp. 29–40.

[13] L. Blanchet and J.-P. Merlet, "Interference detection for cable-driven parallel robots (cdprs)," in *2014 IEEE/ASME International Conference on Advanced Intelligent Mechatronics*. IEEE, 2014, pp. 1413–1418.

[14] G. Xu, H. Zhu, H. Xiong, and Y. Lou, "Data-driven dynamics modeling and control strategy for a planar n-dof cable-driven parallel robot driven by n+ 1 cables allowing collisions," *Journal of Mechanisms and Robotics*, vol. 16, no. 5, 2024.

[15] H. Xiong and Y. Xu, "Statics and path of the cables of a cable-driven parallel robot wrapping on surfaces," in *International Conference on Cable-Driven Parallel Robots*. Springer, 2023, pp. 82–94.

[16] M. Zarebidoki, J. S. Dhupia, and W. Xu, "A review of cable-driven parallel robots: Typical configurations, analysis techniques, and control methods," *IEEE Robotics & Automation Magazine*, vol. 29, no. 3, pp. 89–106, 2022.

[17] T. Rousseau, C. Chevallereau, and S. Caro, "Human-cable collision detection with a cable-driven parallel robot," *Mechatronics*, vol. 86, p. 102850, 2022.

[18] M. Métillon, "Modelling, control and performance analysis of cable-driven parallel cobots," Ph.D. dissertation, Laboratoire des Sciences du Numérique de Nantes - UMR6004, Nantes, June 2023, doctoral research project presented and defended.

[19] M. Métillon, C. Charron, K. Subrin, and S. Caro, "Geometrical modelling of a Cable-Driven Parallel Robot Winch," in *25ème Congrès Français de Mécanique Nantes*, Nantes, France, Aug. 2022.

[20] M. Métillon, L. Rasolofondraibe, R. Gayol, L. Contal, S. Acoulon, C. Charron, K. Subrin, and S. Caro, "A capacitive cable-based detection device for cable-driven parallel robots," Poster presented at CableCon 2023, Nantes, France, June 25-28 2023.